eXPRESS Polymer Letters Vol.15, No.9 (2021) 899–909
Available online at www.expresspolymlett.com
https://doi.org/10.3144/expresspolymlett.2021.72

Carbon dioxide adsorption of diallylamine-modified natural rubber with modified silica particles

D. Tumnantong[1,2], *K. Panploo*[1], *B. Chalermsinsuwan*[1,3], *P. Prasassarakich*[1,2,3], *S. Poompradub*[1,2,3*]

[1]Department of Chemical Technology, Faculty of Science, Chulalongkorn University, 10330 Bangkok, Thailand
[2]Green Materials for Industrial Application Research Unit, Faculty of Science, Chulalongkorn University, 10330 Bangkok, Thailand
[3]Center of Excellence on Petrochemical and Materials Technology, Chulalongkorn University, 10330 Bangkok, Thailand

Received 20 February 2021; accepted in revised form 4 May 2021

Abstract. In this study, modified natural rubber (MNR) was used as a solid adsorbent for carbon dioxide (CO_2) capture. The chemical structure of the NR latex was modified by diallylamine. Moreover, the silica particles were modified by (3-aminopropyl)trimethoxysilane, *N*-[(3-trimethoxysilyl)propyl]ethylenediamine, or *N*-[(3-trimethoxysilyl)propyl]diethylenetriamine (mono-, di- and tri-amines) to improve the CO_2 capture ability of the MNR. The CO_2 adsorption capacity of the MNR foam composite was increased 3- to 5-fold after filling with unmodified or modified silica particles. The mechanism for CO_2 adsorption of the MNR composite was a combination of physisorption and chemisorption. At 100 °C, the highest CO_2 adsorption capacity of MNR foam composite (10.35 mg/g of adsorbent) was obtained by adding tri-amine-modified silica particles. Finally, the MNR foam composite material could be regenerated process for more than 20 CO_2 adsorption cycles.

Keywords: *polymer composites, polymer synthesis, rubber, modified silica, CO_2 adsorption*

1. Introduction

The current dramatic global climate change is mainly caused by the elevated concentration of atmospheric greenhouse gases, especially carbon dioxide (CO_2) [1]. The CO_2 emission forecast from 2018 to 2025 [2] shows a rising concentration of CO_2 in the environment, which is mainly derived from fossil fuel combustion for energy production and transportation. Adsorption processes are one of the CO_2 capture technologies that can effectively reduce the net CO_2 emission rate because of their low-energy requirement, cost-effective method, high CO_2 adsorption capacity, easy regeneration, and can be applied over a wide temperature and pressure range [3, 4]. High porosity materials, including zeolite [5, 6], activated carbon [7, 8], metal-organic frameworks [9], and silica [10, 11], have been used as CO_2 adsorbents. Among the various adsorption materials, silica has been applied the most because of its high surface area, large pore size, and facile surface functionalization [12]. Moreover, incorporating amine species onto the silica surface for enhancing CO_2 capture has also been employed due to the high reactivity and selectivity of amines [13].

Directly introducing tetraethylenepentamine (TEPA) into the mesoporous silica SBA-15 resulted in a high CO_2 adsorption capacity of 173 mg/g of adsorbent [14]. In addition, a mesocellular silica foam material modified by polyethyleneimine (PEI) with the largest window size exhibited a CO_2 adsorption capacity of 152 mg/g of adsorbent [15]. The TEPA-impregnated mesoporous silica also had an increased

*Corresponding author, e-mail: sirilux.p@chula.ac.th

CO_2 adsorption capacity [16]. Accordingly, the use of amine-modified silica to reduce CO_2 emission has attracted attention.

Synthetic polymer foams, such as poly(ethylene-vinyl acetate) [17], poly(ethylene-propylene-diene) [18], acrylonitrile-butadiene rubber [19], and polyurethane foam [20], have gained in interest due to their significant potential in many applications. However, their chemical toxicity and environmental safety are of concern. Therefore, natural rubber (NR) is an alternative to replace these synthetic polymers. NR has good abrasion resistance, but it has poor aging and weathering, which are undesirable properties. Thus, chemical modification of NR has become an important method to improve its otherwise inferior properties [21]. Some hydrophilic monomers have been used to modify the NR latex to improve the interaction between the hydrophilic fillers and the rubbery matrix [22]. Dimethylaminoethyl acrylate [23], dimethylaminoethyl methacrylate [23, 24], and diallylamine [25] have been grafted onto the NR particles. In previous work [26, 27], NR latex foam with amine-modified silica was successfully developed as a CO_2 adsorbent material. NR compounded with modified silica particles was found to enhance the CO_2 adsorption capacity. However, there has been no report on the CO_2 capture in modified NR (MNR). Accordingly, in this study, amine functionalization was used to improve the CO_2 adsorption capacity of NR.

The aim of this study was to modify NR using diallylamine as a CO_2 sorbent material. To enhance the CO_2 adsorption capacity, silica particles modified by (3-aminopropyl)trimethoxysilane (1NM), *N*-[(3-trimethoxysilyl)propyl]ethylenediamine (2NM), or *N*-[(3-trimethoxysilyl)propyl]diethylenetriamine (3NM) were filled in the MNR sorbent material. The functional groups on the MNR structure and on the modified silica surface were confirmed by Fourier-transform infrared spectroscopy (FT-IR). The morphology of the MNR foam composite was examined by scanning electron microscopy (SEM), and the CO_2 adsorption capacity was investigated in a stainless steel reactor under ambient temperature and pressure with a mixed gas flow rate of 50 ml/min. The effect of the temperature on the CO_2 adsorption capacity, kinetic adsorption, and reusability of the MNR foam composite was evaluated. Finally, the mechanism of CO_2 capture on the sorbent material was investigated.

2. Experimental

2.1. Materials

The NR latex with 60% by weight [wt%] of dry rubber content was obtained from the Rubber Research Institute, Thailand. Tetraethyl orthosilicate (TEOS), diallylamine, *t*-butyl hydroperoxide, TEPA, and the three modifiers (1NM, 2NM, and 3NM) were purchased from Sigma-Aldrich, USA. Ammonium hydroxide (NH_4OH; 28.0% purity) and ethanol (EtOH) were purchased from Qrec chemicals, Thailand. Acetone (AR grade) was purchased from Mermaid, Thailand, while *N*,*N*-dinitrosopentamenthylenetetramine (DNT) was supplied from Shaanxi Pioneer Biotech, China. Stearic acid, *N*-cyclohexyl-2-benzothiazole sulfernamide (CBS), sulfur, and zinc oxide were purchased from PAN Innovation, Thailand. All materials were used as received without further purification.

2.2. Modification of NR latex

The MNR was prepared as previously reported [25]. In brief, 100 g of NR latex was diluted with 0.26% (w/w) NH_4OH (37 ml) in a closed glass reactor under a nitrogen (N_2) atmosphere. Then, 5 g of diallylamine in 110 ml of 0.26% (w/w) NH_4OH was added to the reactor and mixed for 30 min under an N_2 atmosphere at room temperature, followed by 1 g of *t*-butyl hydroperoxide (an initiator) and mixed for 15 min at room temperature. Finally, TEPA, as an activator, at 0.5 wt% of rubber was added, and the mixture was heated to 50 °C and maintained with continuous stirring at 50 °C for 24 h. Finally, the MNR was coagulated with acetone and dried at 60 °C in a

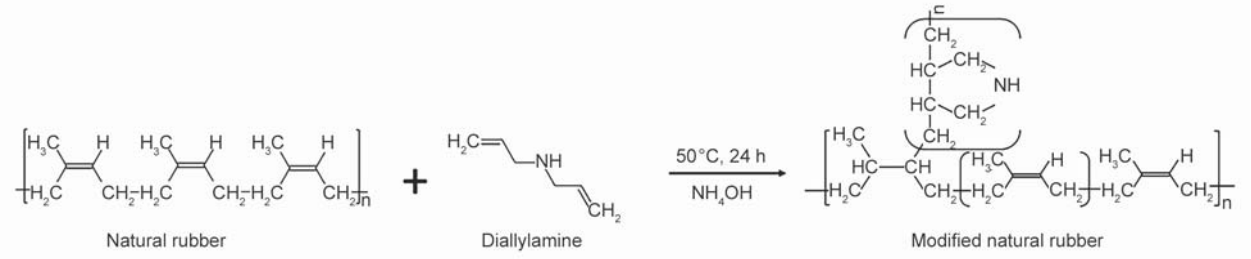

Figure 1. The modification of NR with diallylamine.

vacuum oven. Figure 1 shows the modification of NR by diallylamine.

2.3. Modification of silica particles

The silica particles were modified via a sol-gel reaction by mixing two solutions at ambient temperature [27, 28]. The first solution was a mixture of 3.0 ml TEOS and 23.0 ml EtOH, and the second solution was a mixture of 1.0 ml 28% (w/w) NH_4OH, 7.0 ml deionized (DI) water, and 18.0 ml EtOH. Then, the TEOS modifier (0.4 times by mole composition) was added into the mixed solution and continuously stirred at room temperature for 24 h. For the unmodified silica particles, a similar procedure was performed only without adding the modifier. The silica particles with/without modifier were then separated by centrifugation, and the obtained silica particles were washed by DI water and dried until constant weight. The silica particles modified with 1NM, 2NM, and 3NM were denoted as 1NMSi, 2NMSi, and 3NMSi with the BET surface area of 72.6, 1.8, and 0.1 m^2/g, respectively.

2.4. Preparation of MNR foam composites

The formulation of the rubber compounding is listed in Table 1. All ingredients were mixed in a two-roll mill. The samples were then pressed by a compression mold at 100 °C for 9 min, and then the rubber foam sheet was heated in an oven at 140 °C for 9 min.

2.5. Adsorption of CO_2 by the MNR foam composites

The NR or MNR adsorbent materials in a stainless steel reactor were treated under a vacuum condition at 60 °C for 20 min to remove the adsorbed gas inside the adsorbent material and then cooled down to ambient temperature. Next, N_2 was fed into the stainless steel reactor at a flow rate of 50 ml/min to expel CO_2 from the system, followed by the mixed 12:88 (v/v) CO_2:N_2 at a flow rate of 50 ml/min. This CO_2 percentage is simulated flue gas from coal condition (12–15 vol% CO_2) [29]. The CO_2 concentration and gas temperature at the outlet were detected using a CO_2 sensor.

Table 1. Formulation of rubber compounding.

Ingredient	Function	Weight [phr]
NR or MNR	Substrate	100
Zinc oxide	Activator	4
Stearic acid	Activator	2
CBS[a]	Accelerator	3
DNT[b]	Blowing agent	2
Sulfur	Crosslinking agent	3
Modified silica	Additive	15

[a]*N*-cyclohexyl-2-benzothiazole sulfenamide,
[b]*N*,*N*-dinitrosopentamenthylenetetramine

2.6. Characterization of the MNR and modified silica

N_2 adsorption-desorption isotherms were measured using Micromeritics ASAP-2020 at liquid N_2 temperature (77 K). All samples were degassed at 150 °C for 12 h under evacuation before analysis. The specific surface areas of modified silica particles were evaluated using the Brunauer–Emmett–Teller (BET) method.

The FT-IR spectra of MNR and modified silica particles were recorded at a resolution of 4 cm^{-1} using Nicolet Nexus 670, USA, operating in Attenuated Total Reflectance (ATR) mode with a diamond crystal having a refractive index of 2.4 at the incident angle (θ) of 45°.

The morphology of the NR and MNR filled with/without modified silica particles was examined using SEM (JEPL, JSM-6480LV, Japan) at an acceleration voltage of 15 kV. The samples were first sputter coated with gold under a vacuum to make them electrically conductive.

3. Results and discussion

3.1. Characterization of MNR

Figure 2 shows the FT-IR spectra of diallylamine, NR, and MNR. The characteristic peaks of NR at 2961 and 2853 cm^{-1}, corresponding to the asymmetric stretching of $–CH_3$ and symmetric stretching of $–CH_2$ [30], were evident. Bands at 1664, 1447, and 836 cm^{-1} were assigned to the C=C stretching, $–CH_2$ deformation, and =CH wagging bands of NR, respectively [30]. The inclusion of diallylamine in the MNR increased the absorbance of the N–H stretching vibrations of amine at 3300 cm^{-1} [25], and the spectra at 1642 and 1544 cm^{-1} were assigned to the N–H bending of amine [31]. However, the peaks at 993 and 915 cm^{-1} attributed to the C=C bending of alkene in diallylamine disappeared because the alkene was changed to cycloalkane during the cyclopolymerization, as seen in Figure 1 [31]. Accordingly, the FT-IR results confirmed that the modification of NR was successfully obtained.

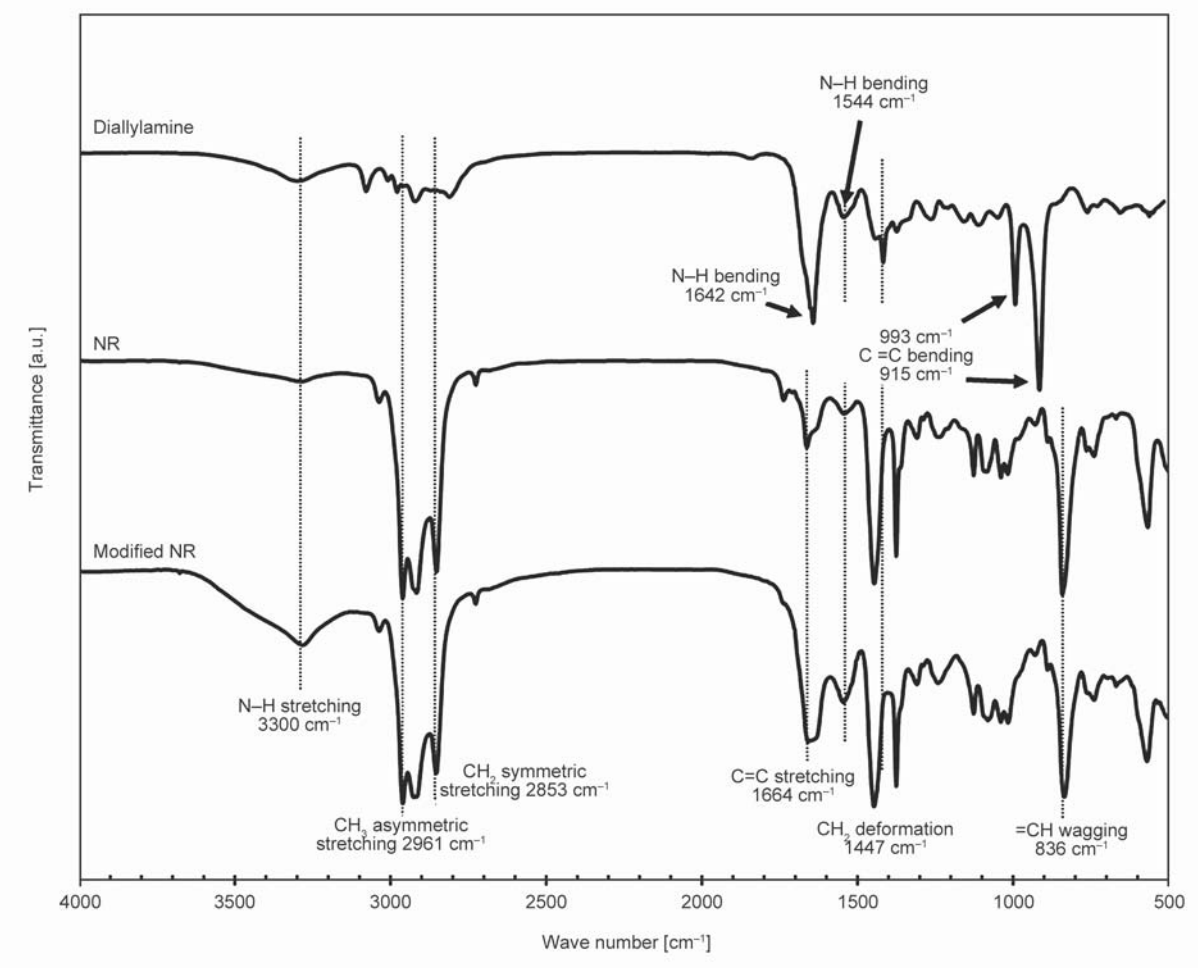

Figure 2. Representative FT-IR spectra of diallylamine, NR, and MNR.

3.2. Characterization of the modified silica particles

The FT-IR spectra of the unmodified and modified silica particles are shown in Figure 3. Unmodified silica particles showed strong signals at 1107 and 802 cm^{-1} associated with the asymmetric and symmetric stretching of Si–O–Si, respectively [32, 33]. The broad band at 948 cm^{-1} was due to the Si–O in-plane stretching vibration in the Si–OH group [33], whilst the peaks at 3434 and 1630 cm^{-1} were attributed to the overlapped band of O–H stretching of physically adsorbed water and the SiO–H stretching of the silanol group [32, 33] and the O–H deformation vibration of the adsorbed water [33], respectively.

After modification, the intensity of the band at 948 cm^{-1} decreased, which indicated that some silanol groups were modified. Moreover, the FT-IR spectra of the modified silica particles showed the stretching and bending vibrations of the aliphatic amine (N–H) groups at about 3400–3300 cm^{-1} and 1630–1680 cm^{-1}, respectively [32]. Unfortunately, these were not evident following the modification of silica by these modifiers because their absorption peaks merged with the peaks of the O–H deformation of water. Compared with the unmodified silica particles, some new peaks appeared at 2945 (asymmetric stretching vibrations), 2881 (symmetric stretching vibrations) and 1480 cm^{-1} (bending vibration) of $–CH_2$ were observed for the amine-modified silica particles [32, 34]. The presence of $–CH_2$ vibrations on the modified silica particles indicated the successful grafting of the amino-organoalkoxyl groups (1NM, 2NM, and 3NM) on the surface of silica.

3.3. Morphology of the MNR foam composite

After successfully preparing either MNR or modified silica particles, the rubber composite material was prepared to obtain the adsorbent material for CO_2 adsorption. Figure 4 shows SEM micrographs of the NR foam, MNR foam, and MNR foam composite filled with unmodified or modified silica particles. Both the NR and MNR foams showed a closed-cell structure, but the cell size of the MNR foam was larger than that of the NR foam. This was because

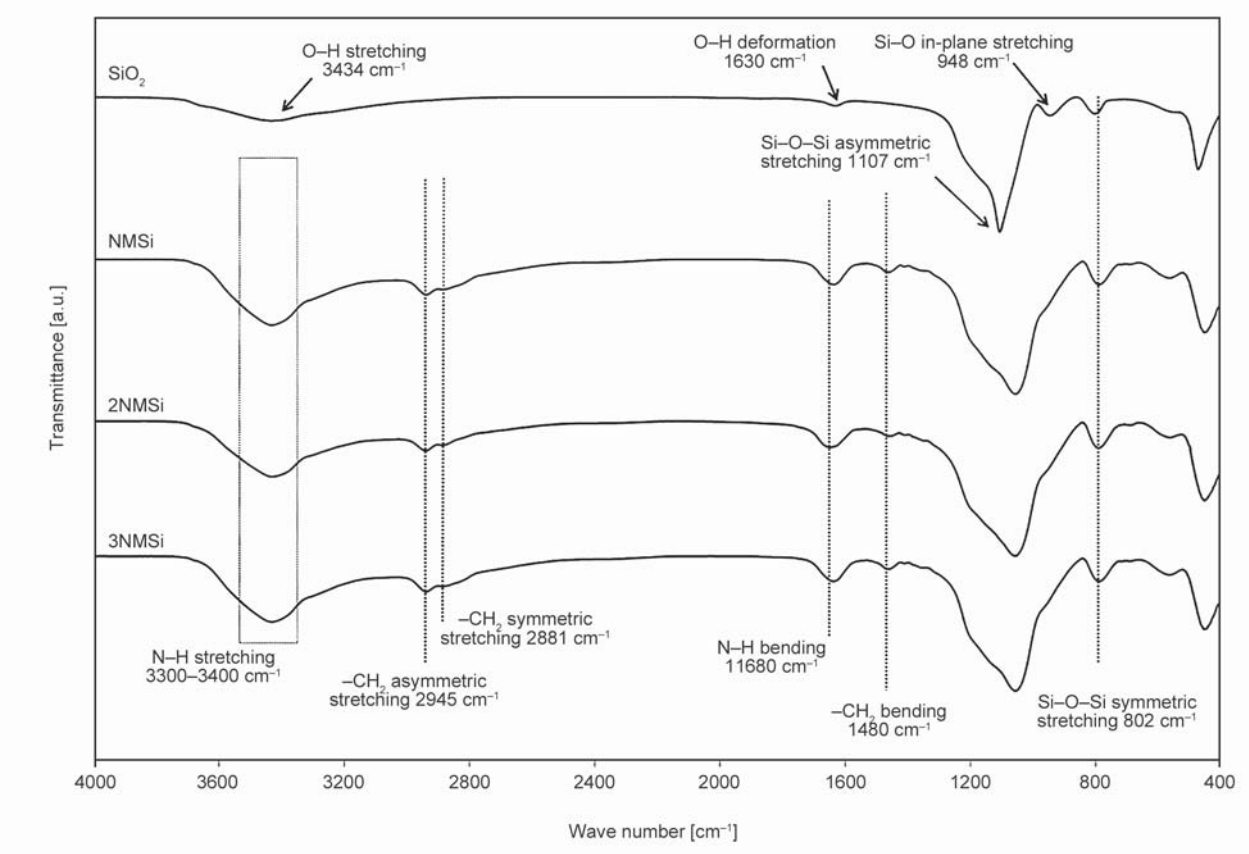

Figure 3. Representative FT-IR spectra of the unmodified and modified (1NM, 2NM, and 3NM) silica particles.

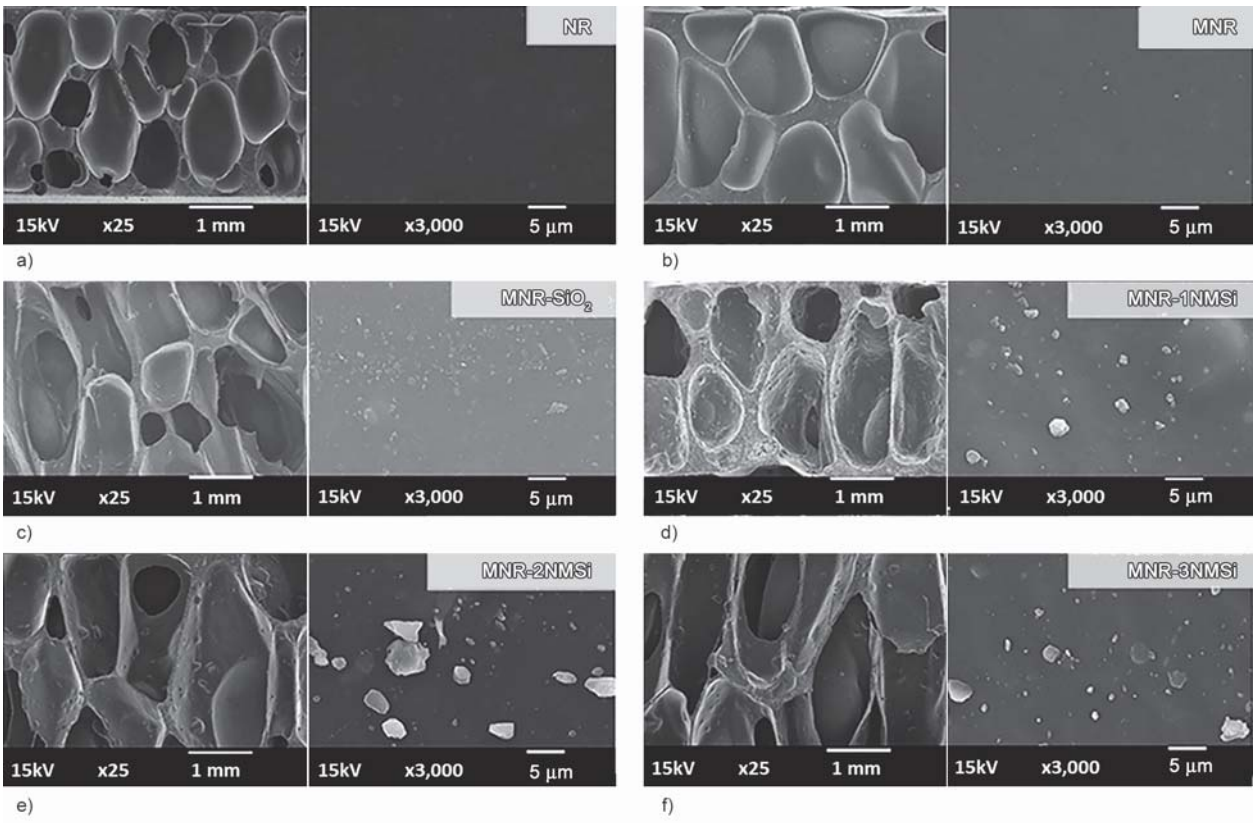

Figure 4. Representative SEM micrographs of the (a) NR, (b) MNR, and (c–f) MNR foam composite filled with (c) unmodified silica or silica modified with (d) 1NM, (e) 2NM, or (f) 3NM.

the increased size of the bulky chain of the MNR structure increased the space in the rubbery matrix, resulting in the foaming agent easily decomposing and forming the larger cell structure. After filling with the SiO_2, the morphology of MNR foam composite was not significantly changed, but the unmodified silica particles showed a good distribution in the rubbery matrix while the modified silica particles tended to be aggregated due to the increased basicity of each modifier. Accordingly, the modifier acted as a catalyst to increase the rate of the sol-gel reaction, resulting in the aggregates or agglomerates of the modified silica particles.

3.4. The CO_2 adsorption capacity

The CO_2 adsorption capacity of the MNR foam composites was investigated at ambient temperature and pressure, and the results are summarized in Table 2. The adsorption capacity of the NR foam was 0.79 mg/g of adsorbent. At the same time, this was ~1.6-fold higher for the MNR foam (1.26 mg/g of adsorbent), which was because of the increased amine groups in the MNR structure that increased the CO_2 selectivity. To further improve the CO_2 adsorption capacity of the MNR foam, unmodified or modified silica particles were then filled in the MNR foam and the effect of the three amine types (mono-, di-, and tri-amine, or 1MN, 2MN, and 3MN, respectively) on the surface of the modified silica particles was evaluated. The CO_2 adsorption capacity of the MNR foam composite was increased from 3- to 5-fold after filling with unmodified to 3MN-modified silica particles (Table 2), owing to the increased surface area and CO_2 selectivity to adsorb CO_2. Moreover, the highest adsorption capacity was achieved using the tri-amine (3MN), which simply reflected the increasing amount of amine units per silane (tri- > di- > mono-). In contrast, in a previous study, the use of the mono-amine showed the highest CO_2 adsorption capacity [27]. This might reflect that the long chain length of the di- or tri-amine silanes could tangle with the NR chains and potentially block many of the secondary amine locations on its tether and so inhibit access for CO_2 capture.

3.5. Kinetics of the CO_2 adsorption on the MNR foam composite

The behavior of CO_2 adsorption process for each adsorbent was compared to the predictions of three models of adsorption kinetics: pseudo-first order, pseudo-second order, and Avrami's models, shown in Equations (1)–(3), respectively [34, 35]:

Pseudo-first order: $$q_t = q_e\left[1 - \exp\left(-k_1 t\right)\right] \quad (1)$$

Pseudo-second order: $$q_t = \frac{k_2 q_e^2 t}{1 + k_2 q_e t} \quad (2)$$

Avrami's: $$q_t = q_e\left[1 - \exp\left(-k_A t\right)^{n_A}\right] \quad (3)$$

where k_1 [min^{-1}], k_2 [g/(mmol·min)], and k_A [min^{-1}] are the respective rate constants, q_e [mmol/g] is the adsorption capacity, q_t [mmol/g] is the amount of gas adsorbed in a specific time t [min], and n_A is the order of the kinetic equation.

The kinetic parameters of these models, along with the coefficient of correlation (R^2) and rate constants, were estimated and are summarized in Table 3. The Avrami's kinetic model fitted well with the adsorption

Table 2. CO_2 adsorption capacity of MNR foam composite material.

Sample code	CO_2 adsorption capacity [mg/g of adsorbent]
NR	0.79
MNR	1.26
MNR-SiO_2[a]	4.29
MNR-1NMSi[b]	5.06
MNR-2NMSi[c]	6.05
MNR-3NMSi[d]	6.11

[a–d]MNR filled with
[a]unmodified silica particles, and silica particles modified with
[b]3-aminopropyltrimethoxysilane (1NM),
[c]*N*-[(3-trimethoxysilyl)propyl]ethylenediamine (2NM),
[d]*N*-[(3-trimethoxysilyl)propyl]diethylenetriamine (3NM).

Table 3. Linear regression parameters for the kinetic data of CO_2 adsorption on the MNR foam composites.

Model parameters		MNR	MNR-SiO_2[a]	MNR-3NMSi[a]
Pseudo-first order	k_1	0.0103	0.0055	0.0072
	R^2	0.9266	0.9336	0.9871
Pseudo-second order	k_2	0.9018	0.4333	0.2488
	R^2	0.5249	0.8791	0.7927
Avrami	k_A	0.0069	0.0061	0.0058
	R^2	0.9896	0.9608	0.9985
	n_A	1.2469	1.0535	1.1351

[a]MNR foam filled with unmodified silica particles or silica particles modified with *N*-[(3-trimethoxysilyl)propyl]diethylenetriamine (3NM).

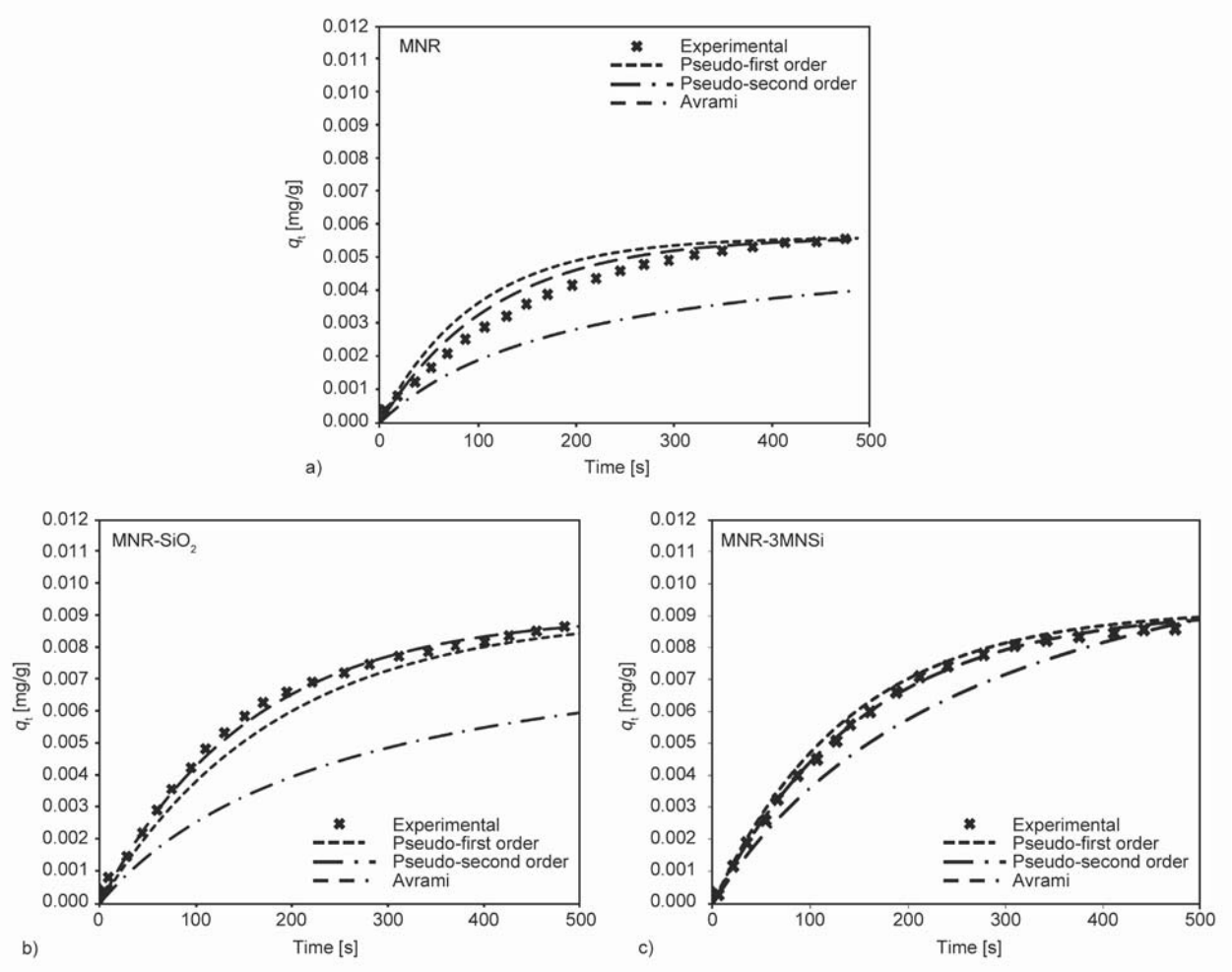

Figure 5. Experimental CO_2 adsorption capacity on the (a) MNR, (b) MNR-SiO_2, and (c) MNR-3NMSi foam composites and the corresponding fit to the different kinetic models.

kinetics data with a high R^2 (>0.95) value, which was consistent with the fitting results (Figure 5). Thus, the CO_2 adsorption mechanism of the MNR foam composite was the combination of physisorption and chemisorption (Figure 6). The n_A of the MNR foam composites was in the range between 1.0535 and 1.2469, which supported a complex reaction mechanism [27, 36]. The physisorption process occurred at the pores of MNR foam or modified silica particles, while the chemisorption occurred from the reaction between CO_2 molecules and amine groups at the MNR structure or on the surface of the modified silica particle surface.

3.6. Effect of temperature on the CO_2 adsorption capacity of the MNR foam composites

The CO_2 adsorption capacity of the MNR foam composites was investigated at various temperatures (ambient temperature, 55, 70, and 100 °C), and the results are summarized in Figure 7. The CO_2 adsorption capacity of the MNR foam tended to increase with increasing temperatures up to 70 °C and then decreased when the temperature was further increased to 100 °C. This was because the structure of the MNR foam might shrink, and the rubber chains would then possibly block the amine groups on the structure. The rubber shrinkage during heating is due to the entropy change (from low to high), hence 'Thermoelastic behavior' [37, 38]. In contrast, the CO_2 adsorption capacity of the MNR foam composites filled with silica and, especially, 3NMSi increased with increasing temperatures up to 100 °C. The addition of filler (silica or 3NMSi) in the MNR foam decreased the volume in the composite, and the resulting structure could not shrink, and so the higher temperature increased the reaction rate. Moreover, the modifier chain on the surface of the modified silica particles became more flexible at a higher temperature, so the active site for CO_2 capture was not hidden.

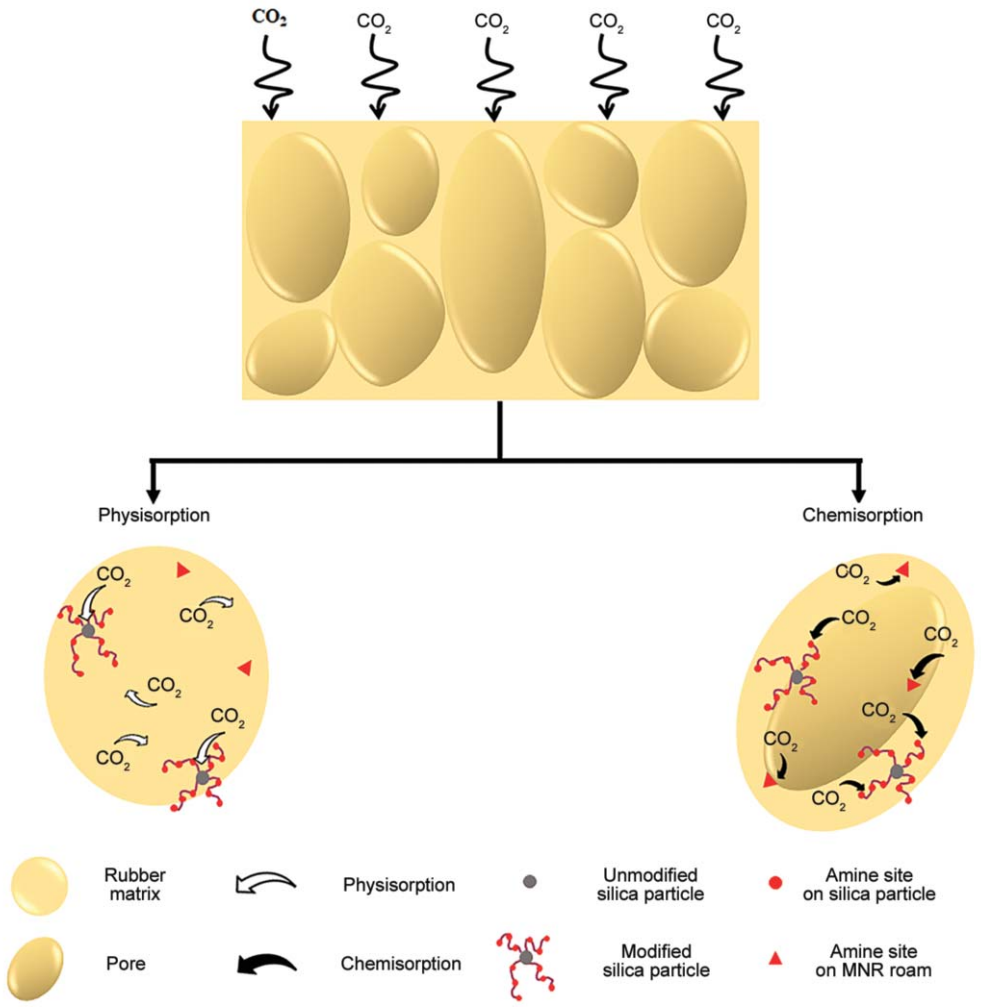

Figure 6. Schematic diagram showing the CO_2 adsorption mechanism on the MNR foam composites.

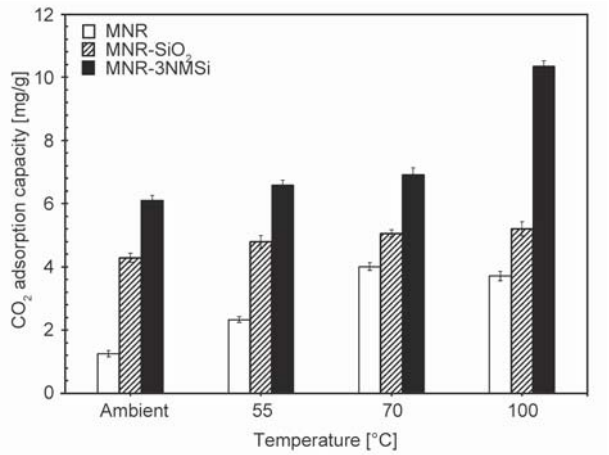

Figure 7. The CO_2 adsorption capacity of the MNR and MNR-SiO_2 and MNR-3NMSi foam composites at different temperatures.

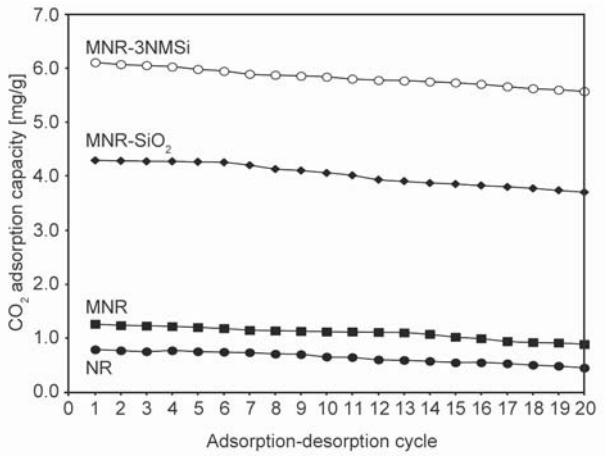

Figure 8. The cyclic CO_2 adsorption capacity of the MNR foam composites.

3.7. Regeneration of the adsorbents

Besides the adsorption behavior, the regeneration behavior is also important for use as an adsorbent material. Figure 8 shows the CO_2 adsorption stability of NR, MNR, MNR-SiO_2, and MNR-3NMSi over 20 successive adsorption-desorption cycles of adsorbing 12% (v/v) CO_2 at ambient temperature and regenerating the adsorbent material at 60 °C under vacuum for 20 min under N_2. For all materials, the CO_2 adsorption capacity slightly decreased with each successive cycle due to decay of the material.

However, after 20 adsorption-desorption cycles, only a maximum 8.3% (in the case of MNR-3NMSi) decreased CO_2 adsorption capacity was observed compared to the fresh adsorbent material. Therefore, it was summarized that the adsorbent materials were stable and could be reused.

4. Conclusions

The MNR was successfully prepared by modification of NR with diallylamine. After curation, the CO_2 adsorption capacity of the MNR foam (1.26 mg/g of adsorbent) was 1.6-fold higher than that of the NR foam (0.79 mg/g of adsorbent) due to the presence of amine groups in MNR structure. The inclusion of amine-modified silica particles further enhanced the CO_2 adsorption capacity of the MNR foam composites. In addition, the CO_2 adsorption capacity of the MNR foam composite material increased depending on the amine type used to modify the silica particles in the order of tri- > di- > mono-amines. The kinetic adsorption of the MNR foam composite fitted well with Avrami's model. Increasing the temperature up to 100 °C increased the CO_2 adsorption capacity of the MNR foam composites, and the MNR foam composites showed high reusability for more than 20 cycles with < 8% loss of CO_2 adsorption. Accordingly, this kind of material could be used as a sorbent material to reduce CO_2 greenhouse gas emissions into the atmosphere.

Acknowledgements

The authors acknowledge the Thailand Research Fund (Grant No. RSA6180030), Malaysia-Thailand Joint Authority (MTJA), Research Cess Fund, the Asahi Glass Foundation, the Center of Excellence on Petrochemical and Materials Technology and the Ratchadapisek Somphot Fund for Postdoctoral Fellowship, Chulalongkorn University.

References

[1] Abeydeera L. H. U.W., Mesthrige J. W., Samarasinghalage T. I.: Global research on carbon emissions: A scientometric review. Sustainability, **11**, 3972/1–3972/25 (2019). https://doi.org/10.3390/su11143972

[2] Qiao W., Lu H., Zhou G., Azimi M., Yang Q., Tian W.: A hybrid algorithm for carbon dioxide emissions forecasting based on improved lion swarm optimizer. Journal of Cleaner Production, **244**, 118612/1–118612/16 (2020). https://doi.org/10.1016/j.jclepro.2019.118612

[3] Dissanayake P. D., You S., Igalavithana A. D., Xia Y., Bhatnagar A., Gupta S., Kua H. W., Kim S., Kwon J-H., Tsang D. C. W., Ok Y. S.: Biochar-based adsorbents for carbon dioxide capture: A critical review. Renewable and Sustainable Energy Reviews, **119**, 109582/1-109582/14 (2020). https://doi.org/10.1016/j.rser.2019.109582

[4] Hussin F., Aroua M. K.: Recent trends in the development of adsorption technologies for carbon dioxide capture: A brief literature and patent reviews (2014–2018). Journal of Cleaner Production, **253**, 119707/1–119707/25 (2020). https://doi.org/10.1016/j.jclepro.2019.119707

[5] Megías-Sayago C., Bingre R., Huang L., Lutzweiler G., Wang Q., Louis B.: CO_2 adsorption capacities in zeolites and layered double hydroxide materials. Frontiers in Chemistry, **7**, 551/1–551/10 (2019). https://doi.org/10.3389/fchem.2019.00551

[6] Murge P., Dinda S., Roy S.: Zeolite-based sorbent for CO_2 capture: Preparation and performance evaluation. Langmuir, **35**, 14751–14760 (2019). https://doi.org/10.1021/acs.langmuir.9b02259

[7] Botomé M. L., Poletto P., Junges J., Perondi D., Dettmer A., Godinho M.: Preparation and characterization of a metal-rich activated carbon from CCA-treated wood for CO_2 capture. Chemical Engineering Journal, **321**, 614–621 (2017). https://doi.org/10.1016/j.cej.2017.04.004

[8] Li M., Xiao R.: Preparation of a dual pore structure activated carbon from rice husk char as an adsorbent for CO_2 capture. Fuel Processing Technology, **186**, 35–39 (2019). https://doi.org/10.1016/j.fuproc.2018.12.015

[9] Hu Z., Wang Y., Shah B. B., Zhao D.: CO_2 capture in metal–organic framework adsorbents: An engineering perspective. Advanced Sustainable Systems, **3**, 1800080/1–1800080/21 (2019). https://doi.org/10.1002/adsu.201800080

[10] Sanz-Pérez E. S., Dantas T. C. M., Arencibia A., Calleja G., Guedes A. P. M. A., Araujo A. S., Sanz R.: Reuse and recycling of amine-functionalized silica materials for CO_2 adsorption. Chemical Engineering Journal, **308**, 1021–1033 (2017). https://doi.org/10.1016/j.cej.2016.09.109

[11] Lee J. J., Yoo C-J., Chen C-H., Hayes S. E., Sievers C., Jones C. W.: Silica-supported sterically hindered amines for CO_2 capture. Langmuir, **34**, 12279–12292 (2018). https://doi.org/10.1021/acs.langmuir.8b02472

[12] Asefa T., Tao Z.: Mesoporous silica and organosilica materials – Review of their synthesis and organic functionalization. Canadian Journal of Chemistry, **90**, 1015–1031 (2012). https://doi.org/10.1139/v2012-094

[13] Chen C., Zhang S., Row K. H., Ahn W-S.: Amine–silica composites for CO_2 capture: A short review. Journal of Energy Chemistry, **26**, 868–880 (2017). https://doi.org/10.1016/j.jechem.2017.07.001

[14] Yue M. B., Chun Y., Cao Y., Dong X., Zhu J. H.: CO_2 capture by as-prepared SBA-15 with an occluded organic template. Advanced Functional Materials, **16**, 1717–1722 (2006). https://doi.org/10.1002/adfm.200600427

[15] Yan X., Zhang L., Zhang Y., Qiao K., Yan Z., Komarneni S.: Amine-modified mesocellular silica foams for CO_2 capture. Chemical Engineering Journal, **168**, 918–924 (2011). https://doi.org/10.1016/j.cej.2011.01.066

[16] Fujiki J., Yamada H., Yogo K.: Enhanced adsorption of carbon dioxide on surface-modified mesoporous silica-supported tetraethylenepentamine: Role of surface chemical structure. Microporous and Mesoporous Materials, **215**, 76–83 (2015). https://doi.org/10.1016/j.micromeso.2015.05.037

[17] Sarver J. A., Sumey J. L., Williams M. L., Bishop J. P., Dean D. M., Kiran E.: Foaming of poly(ethylene-*co*-vinyl acetate) and poly(ethylene-*co*-vinyl acetate-*co*-carbon monoxide) and their blends with carbon dioxide. Journal of Applied Polymer Science, **135**, 45841/1–45841/24 (2018). https://doi.org/10.1002/app.45841

[18] Wang X., Wang Y., Ma L., Guo H., Yang C., Liu N., Wang J.: Design of ethylene-propylene-diene monomer foam and its double-layer composite for improving sound absorption properties *via* experimental method and theoretical verification. Polymer Engineering and Science, **60**, 1877–1889 (2020). https://doi.org/10.1002/pen.25424

[19] Han D-H., Choi M-C., Jeong J-H., Choi K-M., Kim H-S.: Properties of acrylonitrile butadiene rubber (NBR)/poly(lactic acid) (PLA) blends and their foams. Composite Interfaces, **23**, 771–780 (2016). https://doi.org/10.1080/09276440.2016.1170518

[20] Almeida M. L. B., Ayres E., Moura F. C. C., Oréfice R. L.: Polyurethane foams containing residues of petroleum industry catalysts as recoverable pH-sensitive sorbents for aqueous pesticides. Journal of Hazardous Materials, **346**, 285–295 (2018). https://doi.org/10.1016/j.jhazmat.2017.12.033

[21] Phinyocheep P.: Chemical modification of natural rubber (NR) for improved performance. in 'Chemistry, manufacture and applications of natural rubber' (eds.: Kohjiya S., Ikeda Y.) Woodhead, London, 68–118 (2014). https://doi.org/10.1533/9780857096913.1.68

[22] Oliveira P. C., Guimarães A., Cavaillé J-Y., Chazeau L., Gilbert R. G., Santos A. M.: Poly(dimethylaminoethyl methacrylate) grafted natural rubber from seeded emulsion polymerization. Polymer, **46**, 1105–1111 (2005). https://doi.org/10.1016/j.polymer.2004.11.048

[23] Kangwansupamonkon W., Gilbert R. G., Kiatkamjornwong S.: Modification of natural rubber by grafting with hydrophilic vinyl monomers. Macromolecular Chemistry and Physics, **206**, 2450–2460 (2005). https://doi.org/10.1002/macp.200500255

[24] Jayadevan J., Alex R., Gopalakrishnapanicker U.: Chemically modified natural rubber latex – poly(vinyl alcohol) blend membranes for organic dye release. Reactive and Functional Polymers, **112**, 22–32 (2017). https://doi.org/10.1016/j.reactfunctpolym.2017.01.001

[25] Jong L.: Reinforcement effect of soy protein nanoparticles in amine-modified natural rubber latex. Industrial Crops and Products, **105**, 53–62 (2017). https://doi.org/10.1016/j.indcrop.2017.05.007

[26] Panploo K., Chalermsinsuwan B., Poompradub S.: Natural rubber latex foam with particulate fillers for carbon dioxide adsorption and regeneration. RSC Advances, **9**, 28916–28923 (2019). https://doi.org/10.1039/C9RA06000F

[27] Panploo K., Chalermsinsuwan B., Poompradub S.: Effect of amine types and temperature of a natural rubber based composite material on the carbon dioxide capture. Chemical Engineering Journal, **402**, 125332/1–125332/9 (2020). https://doi.org/10.1016/j.cej.2020.125332

[28] Thepppradit T., Prasassarakich P., Poompradub S.: Surface modification of silica particles and its effects on cure and mechanical properties of the natural rubber composites. Materials Chemistry and Physics, **148**, 940–948 (2014). https://doi.org/10.1016/j.matchemphys.2014.09.003

[29] Songolzadeh M., Soleimani M., Takht Ravanchi M., Songolzadeh R.: Carbon dioxide separation from flue gases: A technological review emphasizing reduction in greenhouse gas emissions. The Scientific World Journal, **2014**, 828131/1–828131/34 (2014). https://doi.org/10.1155/2014/828131

[30] Ibrahim S., Daik R., Abdullah I.: Functionalization of liquid natural rubber via oxidative degradation of natural rubber. Polymers, **6**, 2928–2941 (2014). https://doi.org/10.3390/polym6122928

[31] Kadem K. J.: Cyclopolymerization of diallylamine and its condensation with carboxylic drugs. International Journal of Chemical Sciences, **13**, 725–736 (2015).

[32] Lu H-T.: Synthesis and characterization of amino-functionalized silica nanoparticles. Colloid Journal, **75**, 311–318 (2013). https://doi.org/10.1134/S1061933X13030125

[33] Tunlert A., Prasassarakich P., Poompradub S.: Anti-degradation and reinforcement effects of phenyltrimethoxysilane- or *N*-[3-(trimethoxysilyl)propyl]aniline-modified silica particles in natural rubber composites. Materials Chemistry and Physics, **173**, 78–88 (2016). https://doi.org/10.1016/j.matchemphys.2016.01.041

[34] Wang X., Chen L., Guo Q.: Development of hybrid amine-functionalized MCM-41 sorbents for CO_2 capture. Chemical Engineering Journal, **260**, 573–581 (2015). https://doi.org/10.1016/j.cej.2014.08.107

[35] Keramati M., Ghoreyshi A. A.: Improving CO_2 adsorption onto activated carbon through functionalization by chitosan and triethylenetetramine. Physica E: Low-dimensional Systems and Nanostructures, **57**, 161–168 (2014).
https://doi.org/10.1016/j.physe.2013.10.024

[36] Liu Q., Shi J., Zheng S., Tao M., He Y., Shi Y.: Kinetics studies of CO_2 adsorption/desorption on amine-functionalized multiwalled carbon nanotubes. Industrial and Engineering Chemistry Research, **53**, 11677–11683 (2014).
https://doi.org/10.1021/ie502009n

[37] Gedde U. W.: Polymer physics. Kluwer, Amsterdam (1999).

[38] Geethamma V. G., Sampath V.: Rubber as an aid to teach thermodynamics: The discovery by a blind scientist. Resonance, **24**, 217–238 (2019).
https://doi.org/10.1007/s12045-019-0772-x